Food Science and Biotechnology (2024) 33:327–341
https://doi.org/10.1007/s10068-023-01351-9

RESEARCH ARTICLE

Optimization of ultrasound-assisted extraction of bioactive chemicals from *Hemidesmus indicus* (L.) R.Br. using response surface methodology and adaptive neuro-fuzzy inference system

Senthilkumar Vellur[1] · Parasuraman Pavadai[2] · Sureshbabu Ram Kumar Pandian[1] · Chandrasekar Palanichamy[1] · Shanmugampillai Jeyarajaguru Kabilan[1] · Krishnan Sundar[1] · Suthendran Kannan[3] · Selvaraj Kunjiappan[1]

Received: 16 January 2023 / Revised: 13 April 2023 / Accepted: 22 May 2023 / Published online: 17 June 2023

Abstract

This study was designed to optimize the ultrasound-assisted extraction (UAE) of bioactive chemicals from *Hemidesmus indicus* (L.) R.Br. through RSM (response surface methodology) and ANFIS (adaptive neuro-fuzzy inference system). The effect of four independent parameters, methanol concentration (X_1: 55–65%), temperature (X_2: 30–40 °C), time (X_3: 15–20 min) and particle size (X_4: 0.5–1.00 mm) at five levels ($-2, -1, 0, +1, +2$) with respect to dependent parameters, total polyphenols content (TP) (y_1), total flavonoids content (TF) (y_2), %DPPHsc (y_3), %ABTSsc (y_4) and %H_2O_2sc (y_5) were selected. The optimal extraction condition was observed at $X_1 = 65\%$, $X_2 = 40$ °C, $X_3 = 20$ min and $X_4 = 0.5$ mm; under this circumstance, $y_1 = 352.85$ mg gallic acid equivalents (GA)/g, $y_2 = 300.204$ mg rutin equivalents (RU)/g and their antioxidant potentials ($y_3 = 81.33\%$, $y_4 = 65.04\%$, and $y_5 = 71.01\%$) has been attained. ANFIS was used to compare and confirm the optimized extraction parameter values. Further, GC–MS and LC–MS were performed to investigate the bioactive chemicals present in the optimized extract.

Keywords Optimization · RSM · ANFIS · *Hemidesmus indicus* (L.) R.Br. bioactive chemicals

Introduction

Over the last few years, the bioactive chemicals originating from plants and other natural sources have received substantial consideration in the pharmaceutical and healthcare industries due to their therapeutic values (Hosseinzadeh et al., 2015). Many of the plant-derived chemicals have proven their efficacy against several pathological complications, including cancer, neurodegenerative disorders, diabetes mellitus, cardiovascular diseases, inflammation, arthritis, etc. (Forni et al., 2019). It is well established that excessive concentrations of free radicals (reactive oxygen species (ROS), reactive nitrogen species (RNS) and aldehyde-derived DNA adducts (DRA)) leads to numerous complications (Kovacic and Jacintho, 2001). These are potent pro-oxidants/oxidants or reductants because they can speedily lose or gain a single electron (Saetan et al., 2017). The most significant free radicals are generated by our body

✉ Selvaraj Kunjiappan
selvaraj.k@klu.ac.in

Senthilkumar Vellur
v.senthilkumar@klu.ac.in

Parasuraman Pavadai
pvpram@gmail.com

Sureshbabu Ram Kumar Pandian
srkpandian@klu.ac.in

Chandrasekar Palanichamy
p.chandrasekar@klu.ac.in

Shanmugampillai Jeyarajaguru Kabilan
kabilan@klu.ac.in

Krishnan Sundar
sundarkr@klu.ac.in

Suthendran Kannan
k.suthendran@klu.ac.in

[1] Department of Biotechnology, Kalasalingam Academy of Research and Education, Krishnankoil 626126, India

[2] Department of Pharmaceutical Chemistry, Faculty of Pharmacy, M.S. Ramaiah University of Applied Sciences, M S R Nagar, Bengaluru 560054, India

[3] Department of Information Technology, Kalasalingam Academy of Research and Education, Krishnankoil 626126, India

during metabolic or physicochemical processes as unavoidable by-products, and these radicals are made up of oxygen, nitrogen and aldehydes (Valko et al., 2006). Free radicals have a dual role with both beneficial and toxic consequences. They are reactive atoms, and their outer shell typically contains one or more unpaired electrons (Vellur et al., 2023). At a lower concentration, free radicals are necessary for several metabolic processes as well as regulatory mediators in cell signaling events (Ganesan et al., 2018). At higher concentrations the free radicals leads to oxidative damage, which harms the cell irreparably (Burton and Jauniaux, 2011). For normal physiological function, the level of free radicals and antioxidants must coexist in balance (Valko et al., 2007). The excessive production of free radicals is mainly caused by exposure due to X-rays, industrial chemicals, ultraviolet radiation, environmental pollutants, cigarette smoking with excessive consumption of alcohol, consumption of repeated heated vegetable oils, high doses of NSAID (non-steroidal anti-inflammatory drugs), and chronic infections (Lobo et al., 2010). Flavonoids, glycosides, steroids, and quinones are polyphenolic chemicals found in plant secondary metabolites that scavenge free radicals to prevent other molecules from oxidizing Particularly, flavonoids are attractive due to their biological activities, and prevent/neutralize the excessive generation of free radicals (Selvaraj et al., 2014). Plant-derived molecules also enhance the antioxidant-defense mechanisms against oxidative stress (Zhou et al., 2018).

Hemidesmus indicus (L.) R.Br., a twining plant of the Asclepiadaceae family, generally called "Indian Sarsaparilla" has been used in Siddha, Ayurvedic, and Unani medicinal systems to treat inflammation, blood disorders, and other ailments (Vellur et al., 2023). The root part of *H. indicus* (L.) R.Br. is used as a coolant for the preparation of traditional medicines and soft drinks, as well as blood-purifier (Kharat and Mokat, 2020). The root is also used in the fourth and ninth month of pregnancy to prevent miscarriage (Jayalakshmi et al., 2018). Numerous research reported that the chemical composition of the root extract of *H. indicus* (L.) R.Br. contains phytochemicals (2-hydroxy-4-methoxy-benzoic acid, b-sitosterol, α- and β-amyrins, nerolidol, caryophyllene, ferulic acid, isoquercitrin, caffeic acid, gallic acid, borneol, lupeol, tetracyclic triterpene alcohols, hemidesminin, hemidesmin-1 and 2, resin acids, fatty acids, tannins, glycosides and a ketone, etc.) that are used to treat several complications (Boominathan et al., 2018; Deshmukh et al., 2019; Nayar et al., 1978). The extraction and purification of these bioactive compounds from *H. indicus* (L.) R.Br. is unquestionably the most challenging technological operation is required because of their extremely low abundance and thermosensitivity.

In order to obtain full extractions of polyphenolic compounds from plant sources, researchers make use of a variety of different extraction procedures. (Selvaraj et al., 2022). In addition to being effective, an extraction method for bioactive chemicals from plant materials should also be risk-free, easily accessible, and cost-effective, all while requiring a less amount of solvent and being gentler on the environment. According to this perspective view, ultrasound-assisted extraction (UAE) using conventional solvent systems is one of the better options for extracting the bioactive compounds as much as possible from plant sources. The UAE method is one of the preferred methods, as this consumes lesser amount solvents, takes shorter extraction time, can be performed at lower temperatures, needs less energy and the possibility of automation. This also results in higher yield of bioactive chemicals as compared to other extraction techniques (Selvaraj et al., 2022). In light of the information presented above, the primary objective of this research is to extract bioactive chemicals from *H. indicus* (L.) R.Br., while also taking into account the efficient extraction parameters. These parameters include things like solvent type and concentration, ultrasonic intensity, particle size, temperature, time, pulse cycle/mode, pH, and other factors that have a significant influence on the extraction yield of polyphenolic compounds and their antioxidant potentials. The optimal setting for each of these extraction parameters must be determined in order to obtain the highest possible yield. In this case, an effective statistical tool, Response Surface Methodology (RSM), was utilized to analyze the ideal conditions to enhance the yield of bioactive polyphenolic compounds while minimizing time, using the solvent efficiently, and reducing the number of tests (Chowdhury et al., 2018).

RSM is a group of designed experiments with statistical methods that are used to establish and concurrently solve multivariate equations by measuring the linear, interaction and quadratic terms from extraction experiments (Ganesan et al., 2018). RSM typically employs a second polynomial order equation fit to construct a model between the dependent and independent responses, and then uses that model to create a symmetrical one that predicts and identifies the experimentally best conditions (Baskararaj et al., 2019). The central composite design (CCD) and the Box–Behnken design (BBD) are frequently considered strategies for the use of RSM to acquire the optimal extraction conditions for the maximum yield of bioactive polyphenolic chemicals from plant sources (Chowdhury et al., 2013). The rotatable central composite design (RCCD) has been employed in numerous research work for the extraction of antioxidants and bioactive polyphenolic compounds (Ganesan et al., 2018). The resulting optimal conditions are also predicted using the ANFIS model, which can yield the best outcomes for nonlinear systems (Chowdhury et al., 2018). It makes use of the computer systems of neural networks and highly sophisticated fuzzy systems that mimic human thinking. ANFIS is an intelligent neuro-fuzzy technique applied to research how factors interact and have nonlinear effects (Al-Mahasneh et al., 2016).

Five coded levels (−2, −1, 0, +1, +2), four parameters (solvent concentration (%), temperature (°C), time (minutes), and particle size (mm)), and an ANFIS model were used to optimize the total polyphenols content (TP), total flavonoids content (TF), and antioxidant scavenging capacity.

Materials and methods

Plant material

H. indicus (L.) R.Br., known as "Indian Sarsaparilla", was obtained in June 2022 from the Western Ghats slopes in and near Kilavankovil Hills (longitude: 77.5232° and latitude: 9.6383°), Virudhunagar district, Tamil Nadu, India. A fine knife separated the plucked plant's root. The separated roots dried naturally for five days after being cleaned with potable water to remove dirt and other debris. Mixer grinders crushed the totally dried roots into a fine powder, while sieves screened the requisite powder sizes (0.25, 0.5, 0.75, 1 and 1.25 mm). (Mesh No. 60, 35, 25, 18, and 16, respectively). The powder samples (moisture: 10 ± 2%) were stored in a desiccator until the experiment.

Materials

From Sigma-Aldrich in St. Louis, Missouri, USA, we ordered 2,2-diphenyl-1-picrylhydrazyl (DPPH) and 2,2′-Azinobis (3-ethylbenzothiazoline-6-sulphonic acid) (ABTS). The following chemicals were provided by HiMedia labs Pvt. Ltd., Mumbai, India: methanol, FCR reagent (Folin-Ciocalteu's phenol), sodium carbonate, sodium nitrite, aluminum chloride, hydrogen peroxide, rutin, ascorbic acid, and gallic acid.

Extraction of bioactive metabolites

Using an ultrasound-assisted extractor (UAE), the bioactive metabolites were isolated from the fine powder of *H. indicus* (L.) R.Br. The experimental device has a ultrasonic water bath (temperature precision of ± 1.0 °C, power 220 V, and continuous mode at 20 kHz high-intensity ultrasound processor) including a jacketed reactor with 250 mL capacity. (Constructed by PCI Analytics Ltd., Mumbai, India). The analysis of the metabolites was conducted using a Shimadzu UV-1800 series UV–Visible spectrophotometer using UV Probe 2.62 software from Japan.

Preliminary experiments to choose the best solvent system

The primary goal of the preliminary studies was to determine the optimal solvent solution by maximizing the contents of TP (total polyphenols content), TF (total flavonoids contents) and antioxidant ability (DPPH* scavenging) of *H. indicus* (L.) R.Br. extract. The selection of the ideal solvent is crucial for solvent extraction. Seven solvents, namely ethanol, methanol, isopropanol, ethyl acetate, diethyl ether, chloroform, and n-hexane are selected for this study. Later, the extraction was performed in each solvent system (20 mL with 70% v/v in water) with *H. indicus* (L.) R.Br. fine powder (2 g), at fixed parameters (0.2 pulse cycle, 60 W/cm^2 ultrasound intensity, 0.5 mm particle size, and 65 °C).

Selection of UAE parameters

The four independent extraction parameters, namely solvent concentration (55–65% v/v in water; X_1), temperature (30–40 °C; X_2), time (15–20 min; X_3) and particle size (0.5–1.0 mm; X_4) were chosen in consideration of the dependent parameters, such as, TP, TF, DPPH, ABTS, and H_2O_2 radicals scavenging ability of *H. indicus* (L.) R.Br. root extract. Furthermore, methanol was chosen as a solvent system for the extraction process according to the preliminary experimental results, as shown in Supplementary Table 1.

Ultrasound-assisted extraction (UAE)

A 2 g fine-powered sample of *H. indicus* (L.) R.Br. in 20 mL of methanol was subjected to UAE using a flexible ultrasonic bath extractor at the predetermined temperature, time, with fixed ultrasound intensity (60 W/cm^2), and pulse cycle. (0.2). All experiments were carried out at least three times, according to the RCCD of RSM. After extraction, the liquid was filtered through Whatman No. 1 filter paper and centrifuged at 2600×*g* for 5 min. After collecting the supernatant (extract), we used a rotary vacuum drier (Varian Rotavac) to concentrate it at 40 °C before testing it for total phenols, total flavonoids, and antioxidant capacity.

Estimation of total polyphenols content (TP)

The Folin-Ciocalteu method was modified to measure the total polyphenols in dried extract samples Singleton et al. (1999) 0.3 mL of each extract was combined with 1.8 mL of FCR reagent. After 5 min, 1.2 mL of sodium carbonate (7.5%, w/v) was added to the mixture and incubated for 90 min in darkness. The extract was replaced with distilled water. UV–Visible spectrophotometers measured absorbance at 765 nm. The results were given in mg gallic acid equivalents per gram of dry extract (GA/g). Each experiment was conducted three times to ensure measurement consistency.

Estimation of TF

The modified approach was used to measure each extract sample's total flavonoids Siddhuraju and Becker (2003). Briefly, 1 mL of each extract was mixed with 0.3 mL of 5% (w/v) sodium nitrite solution, 4 mL of 80% methanol (v/v in water), and 0.3 of 10% aluminium chloride solution. After 6 min, 3 mL of 1 µL sodium hydroxide was added. Vortexed mixture absorbance was 510 nm. The standard curve was prepared using rutin, and the TF concentration findings were expressed as mg RU/g of dry extract.

Measurement of antioxidant potential of the extract

DPPH* scavenging assay

The DPPH assay was utilized in order to test the anti-oxidant potential of the extract. The evaluation of the assay was carried out in accordance with the methodology described by Brand-Williams et al. (1995) with a few modifications. An aliquot of 0.1 ml of each sample of extract was mixed with three milliliters of ethanolic solution containing DPPH. After vigorously shaking the reaction mixture, it was left to incubate in the dark for a period of thirty minutes. The absorbance was measured at a wavelength of 517 nm in comparison to a blank. The formula was used to determine a substance's capacity to scavenge free radicals measured in DPPH as %DPPHsc. (1):

$$\%\mathrm{DPPHsc} = \left(\mathrm{A}_0 - \mathrm{A}_1\right) \times 100/\mathrm{A}_0 \quad (1)$$

where A_0 = absorbance of the control; A_1 = absorbance of the sample.

ABTS* scavenging assay

With minor adjustments Selvaraj et al. (2013) employed the ABTS free radical-scavenging assay (%ABTSsc) to test the scavenging ability of each H. indicus (L.) R.Br. extract. Incubation of 7 mM ABTS solution and 2.45 mM potassium persulphate ($K_2S_2O_8$) solution in the dark at room temperature for 16 h produces ABTS radical cations. To get an absorbance of 0.700 (±0.0020) at 734 nm, dilute the ABTS solution with 0.3 mL ethanol and mix it with 0.1 mL of the extracts. A spectrophotometer measured the reaction mixture's absorbance at 734 nm after 6 min. The formula was used to calculate the %ABTS scavenging ability of rutin in 80% ethanol. (2):

$$\%\mathrm{ABTSsc} = \left(\mathrm{A}_0 - \mathrm{A}_1\right) \times 100/\mathrm{A}_0 \quad (2)$$

where A_0 = absorbance of the control; A_1 = absorbance of the sample.

H_2O_2* scavenging assay

The referred procedure from Ruch et al. (1989) was adjusted to determine each extract's H_2O_2 radical scavenging activity. After adding 0.6 mL of H_2O_2, 0.1 mL of each extract was placed in Eppendorf tubes. The tubes were filled with 50 mM phosphate buffer at pH 7.4 to 0.4 mL. The reaction mixture was vortexed and spectrophotometrically measured at 230 nm after 10 min of incubation. Ascorbic acid was the positive control and the percentage of free radical-scavenging was calculated using the following Eq. (3):

$$\%\mathrm{H_2O_2sc} = \left(\mathrm{A}_0 - \mathrm{A}_1\right) \times 100/\mathrm{A}_0 \quad (3)$$

where A_0 = absorbance of the control; A_1 = absorbance of the sample.

Experimental design and parameters optimization using RSM

The RSM based on RCCD was used to explore the optimization of effective extraction parameters using UAE. To determine the most efficient way to extract the bioactive polyphenolic components from *H. indicus* (L.) R.Br., four independent parameters (X_1, X_2, X_3, and X_4) were chosen, and were examined at five coded levels, as −2, −1, 0, +1, and +2 (as presented in Table 1). It consists of thirty experimental combinations including sixteen factorial and eight axial points (α) placed at a distance of ±2 from the centre. Table 2 displays six replicates of the central points. The independent parameters were coded based on the below Eq. (4)

$$x_i = \frac{Xi - Xz}{\Delta Xi} \quad i = 1, 2, 3 \ldots K \quad (4)$$

Table 1 Experimental range of coded and actual values for central composite rotatable design (CCRD)

Independent variables (xj)	Symbol	Factor levels				
		−2	−1	0	+1	+2
Methanol concentration (%)	X_1	50	55	60	65	70
Temperature (°C)	X_2	25	30	35	40	45
Time (min)	X_3	12.5	15	17.5	20	22.5
Particle size (mm)	X_4	0.25	0.5	0.75	1	1.25

Table 2 Central composite rotatable design with experimental responses and predicted responses

Run	Independent parameters				Experimental responses*					RSM predicted responses					ANFIS predicted responses				
	X_1	X_2	X_3	X_4	y_1	y_2	y_3	y_4	y_5	y_1	y_2	y_3	y_4	y_5	y_1	y_2	y_3	y_4	y_5
1	65	30	20	0.5	298.85	280.449	65.6667	50.8287	54.5	276.579	245.881	59.567	48.227	51.331	299	280	65.7	50.8	54.5
2	65	40	15	1	240.35	222.626	52.5556	48.0884	40.9091	235.0829	216.318	61.4087	52.0387	47.9781	240	223	52.6	48.1	40.9
3	65	30	15	1	236.35	212.543	86.6667	65.93	70.7273	221.746	181.156	66.4976	53.0654	64.3436	236	213	86.7	65.9	70.7
4	65	40	20	1	239.85	216.503	61.6667	49.9834	53.2338	228.913	213.159	50.1596	38.897	40.0114	240	217	61.7	50	53.2
5	60	35	17.5	0.25	312.35	290.578	78.8889	73.267	66.4935	280.392	252.395	50.242	41.611	49.372	312	300	78.9	73.3	66.5
6	55	40	20	1	182.85	173.374	37.7778	31.3517	25.1948	194.913	172.3	34.2465	30.1568	29.3309	183	173	37.8	31.4	25.2
7	55	30	20	1	205.85	188.395	51.2222	45.5912	30.5195	185.579	163.685	42.8359	39.3518	29.1629	206	188	51.2	45.6	30.5
8	60	35	17.5	0.75	276.85	258.235	60.7778	50.6133	54.5455	212.1	183.376	43.7778	36.9408	39.1126	274	258	58.8	48.7	52.8
9	60	35	17.5	0.75	273.35	262.558	58.345	48.6231	52.324	212.1	183.376	43.7778	36.9408	39.1126	274	258	58.8	48.7	52.8
10	70	35	17.5	0.75	324.85	297.66	86.2222	66.1657	72.2857	377.892	342.163	97.0939	77.0813	87.7898	325	298	86.2	66.2	72.3
11	55	40	15	1	209.85	178.748	44.4444	38.0092	39.6104	183.329	159.269	34.9744	30.2524	26.1044	210	179	44.4	38	39.6
12	60	25	17.5	0.75	111.85	101.673	34.2222	27.8232	17.5325	140.058	124.072	37.3391	29.9407	22.201	112	102	34.2	27.8	17.5
13	60	35	17.5	0.75	270.35	256.451	61.453	48.345	52.342	212.1	183.376	43.7778	36.9408	39.1126	274	258	58.8	48.7	52.8
14	55	40	15	0.5	101.85	92.9252	20	16.1694	15.3247	154.079	130.074	23.2235	20.2235	23.1707	102	92.9	20	16.2	15.3
15	60	35	17.5	0.75	279.85	254.432	57.367	48.452	53.456	212.1	183.376	43.7778	36.9408	39.1126	274	258	58.8	48.7	52.8
16	65	40	20	0.5	352.85	300.204	81.3333	65.035	71.013	332.413	282.36	80.3531	62.2167	69.1134	336	291	81.3	65	71
17	60	45	17.5	0.75	167.35	140.585	36	28.14	15.0649	178.725	155.878	42.9457	34.297	26.9316	167	141	36	28.1	15.1
18	50	35	17.5	0.75	246.85	215.075	43.8889	41.1934	39.7403	233.392	208.264	43.0798	38.5524	40.7714	247	215	43.9	41.2	39.7
19	55	30	15	0.5	192.35	195.415	22.2222	13.4254	17.6623	154.496	144.299	18.1596	14.1532	14.2105	192	195	22.2	13.3	17.7
20	65	30	15	0.5	267.85	219.497	47.2222	40.663	54.5455	264.996	236.926	56.2606	43.9414	50.5484	268	219	47.2	40.7	54.5
21	55	40	20	0.5	246.35	193.17	40	36.6114	59.7403	210.663	168.093	43.6411	37.993	48.3663	246	193	40	36.6	59.7
22	60	35	17.5	0.75	272.35	256.532	56.348	47.625	52.5214	212.1	183.376	43.7778	36.9408	39.1126	274	258	58.8	48.7	52.8
23	60	35	17.5	0.75	268.85	260.52	58.456	48.601	51.3401	212.1	183.376	43.7778	36.9408	39.1126	274	258	58.8	48.7	52.8
24	60	35	22.5	0.75	129.85	102.218	21.1111	19.0608	16.2338	173.475	137.226	33.5428	29.6212	30.727	130	102	21.1	19.1	16.2
25	55	30	15	1	170.85	126.367	36.6667	31.9834	33.1169	200.496	163.941	50.1539	39.8852	39.1556	171	126	36.7	32	33.1
26	60	35	12.5	0.75	154.35	112.558	33.3333	27.7164	24.6753	150.308	115.241	30.9643	25.4306	26.7173	154	113	33.3	27.7	24.7
27	60	35	17.5	1.25	204.35	188.748	43.3333	34.0939	41.5584	222.892	203.249	52.0428	44.0241	45.2151	204	189	43.3	34.1	41.6
28	55	30	20	0.5	170.85	146.367	35.3333	33.3517	33.1169	184.579	169.031	31.9872	31.4849	26.187	171	146	35.3	33.4	33.1
29	65	40	15	0.5	322.85	289.456	77.64	61.6114	70.4286	294.329	260.118	70.4567	57.4927	55.1109	323	289	77.6	61.6	70.4
30	65	30	20	1	232.85	188.333	47.3333	42.582	51.9481	189.829	167.54	49.6169	40.6115	44.2411	233	188	47.3	42.6	51.9

*All the experiments were repeated three times

where x_i is the dimensionless value of the independent parameter; Xi, the real value; Xz, the real value at the center point; and ΔXi, a step change in the real value of the parameter i representing a variation of a unit for the dimensionless value. Equation determined the number of experiments (5).

$$N = 2^K(\text{factorial points}) + 2k\ (\text{axial points}) + n_0(\text{central points}) \quad (5)$$

A design with 30 experimental combinations has N experimental runs, k independent parameters, and n_0 central point duplicates. A second polynomial order model was used to determine the correlation between the experimental variable and response variable. The RSM model is as follows (Eq. 6):

$$Y = \beta_0 + \sum_{i=1}^{3} \beta_i X_i + \sum_{i=1}^{3} \beta_{ii} X_i^2 + \sum_{i=1}^{2} \sum_{j=i+1}^{3} \beta_{ij} X_i X_j + \varepsilon \quad (6)$$

Based on the value of four parameters, the Eq. (7) could be converted as given below:

$$\begin{aligned} Y = {} & \beta_0 + \beta_1 X_1 + \beta_2 X_2 + \beta_3 X_3 + \beta_4 X_4 + \beta_{12} X_1 X_2 \\ & + \beta_{13} X_1 X_3 + \beta_{14} X_1 X_4 + \beta_{23} X_2 X_3 + \beta_{24} X_2 X_4 \\ & + \beta_{34} X_3 X_4 + \beta_{11} X_1^2 + \beta_{22} X_2^2 + \beta_{33} X_3^2 + \beta_{44} X_4^2 \end{aligned} \quad (7)$$

where Y is the studied parameters (TP (y_1), TF (y_2), %DPPHsc(y_3), %ABTSsc (y_4) and H_2O_2sc(y_5), β_0 represents the constant of the model, β_i, β_{ii}, and β_{ij} are the linear, interactive and quadratic coefficients, respectively. X_i and X_j are coded value of independent parameters, and ε is an error term. Five additional tests were then performed to statistically validate the extraction parameter in accuracy.

Optimization using ANFIS modelling

Artificial neural networks (ANN) and fuzzy inference systems (FIS) are two types of hybrid soft computing systems that are used in adaptive neuro-fuzzy inference systems, generally known as adaptive network-based fuzzy inference systems (ANFIS). Jang made the suggestion in 1993 using the Takagi–Sugeno fuzzy inference technique. This technology has garnered a lot of interest and is frequently used for a wide range of issues, including statistical optimization procedures. It is utilised for input and output variable relationships that are both linear and non-linear. Additionally, our system modelled the provided training datasets using least squares and back propagation. ANFIS starts by employing back propagation of ANN to train the data. Following that, fuzzy logic membership functions for the input parameters of methanol concentration (X_1), temperature (X_2), time (X_3), and particle size (X_4) will be employed with the ANN's output. FIS is utilised to improve the accuracy of these parameters' optimization. The individual predicted output of TP (y_1), TF (y_2), and antioxidant activities (DPPH*sc (y_3), ABTS*sc (y_4), and H_2O_2*sc (y_5)) was examined using the optimization by ANFIS modelling and comparable RCCD of RSM experimental data. The first-order Takagi–Sugeno–Kang (TSK) model was utilised in the ANFIS for multiple inputs (X_1, X_2, X_3, and X_4) and only produced one output at a time (y_1/y_2/y_3/y_4/y_5). An ANFIS model's functional block diagram (Supplementary Fig. 1) depicts four inputs and one output at a time. The number of rules and antecedent membership functions are determined using the ANFIS rule for successful extraction of polyphenolic compounds, and then linear least squares estimation is used to find each rule's ensuing equations. If we consider a Sugeno Fuzzy Inference System (FIS), which has two inputs namely 'a' and 'b' and one output as 'c'. A first order Sugeno FIS has the rules as following:

Rule1: If a is D_1 and b is E_1, then $f_1 = r_1a + s_1b + t_1$
Rule2: If a is D_2 and b is E_2, then $f_2 = r_2a + s_2b + t_2$

The number of membership functions in each input variable is decided using the trial-and-error method. The experimental data were separated into training, testing, and validation of the network model to predict the outcome of the extraction of polyphenolic chemicals from *H. indicus* (L.) R. Br. using the fuzzy logic toolbox in MATLAB version R2013a.

Validation of optimized parameters and predictive models

To ensure the accuracy of the optimization outcome, the suitability of verification experiments was tested. Three replicate experiments employing combinations of responses with the smallest differences were carried out under ideal circumstances in order to evaluate the model's logic. The predicted values and the mean experimental values were then contrasted.

GC–MS and LC–MS analysis

The phenolic compounds profile of the obtained extract under optimized conditions from *H. indicus* (L.) R.Br. have been explored with gas chromatography-mass spectroscopy and liquid chromatography-mass spectroscopy for the volatile and non-volatile compounds respectively. According to our previously described procedure, the extract was analyzed by GC–MS using a Shimadzu QP-2010 equipped with a non-polar 60 M RTX 5MS column (Baskararaj et al., 2019). The chemical components from the optimized extract of *H. indicus* (L.) R.Br. were identified by comparing the retention times (min) of chromatographic peaks. In order to identify the mass spectral patterns, the size and height of the peak as measured by the quadrapole detector were compared to the NIST 2014 library (National Institute of Standards and

Technology 2014). According to the procedure we previously stated, the LC–MS analysis was carried out utilizing the 1290 Infinity UHPLC System, 1260 Infinity Nano HPLC with Chipcube, and 6550 iFunnel Q-TOFs (Agilent Technologies, USA) (Chowdhury et al., 2018).

Statistical data analysis

All experimental runs were performed according to the RCCD of RSM and were repeated three times. Design Expert software (trial version 8.0.7.1, Stat-Ease, Inc., 2021 East Hennepin Ave, Suite 480, Minneapolis, MN 55413, USA) was used to examine the experimental design, data analysis, and analysis of the development of the quadratic model. The R^2 (regression coefficient) value was applied to measure the goodness of fit of the model. Further, the statistical analysis was assessed by using one-way analysis of variance (ANOVA), with p-values less than 0.05 were considered as significant. The ideal extraction parameters were used to produce 3D (three-dimensional) response surfaces and 2D (two-dimensional) contour plots. For statistical analysis, Microsoft Excel 2016 and the MATLAB (Mathematical Laboratory) version R2013a software and adaptive neuro-fuzzy logic toolbox were also used.

Result and discussion

Fitting the model

The UAE is a significant extraction method that provides numerous advantages such as faster extraction of phytochemicals from natural sources, lesser consumption of solvents, simplified operation, higher reproducibility, with low temperature and lower energy input. In this study, the effective extraction of bioactive chemicals from *H. indicus* (L.) R.Br. the four independent extraction parameters, such as methanol concentration (X_1), temperature (X_2), time (X_3) and particle size (X_4) were optimized through RCCD in RSM. The experimental design tabulated for the combinations of UAE process variables with extraction parameters to study their linear, interaction and quadratic effect on the highest yield of bioactive polyphenolic compounds from *H. indicus* (L.) R.Br. The TP, TF, and antioxidant potentials (%DPPHsc, %ABTSsc, and $\%H_2O_{2sc}$) in UAE of *H. indicus* (L.) R.Br. under various experimental settings are depicted in Table 2, together with their experimental and predicted values. According to the findings, the optimal values were attained at a methanol concentration of 65%, at a temperature of 40 °C, a time 20 min and a particle size of 0.50 mm. In this condition, 352.85 mg GA/g and 300.204 mg RU/g were shown to be the best yields of TP and TF. It was obtained to have 81.33% DPPHsc, 65.03% ABTSsc, and 71.01% H_2O_2sc potential of antioxidants. The reason behind the highest yield of bioactive compounds and antioxidant potentials might be a combination of appropriate solvent, solvent concentration, temperature, time with ultrasonic waves. These results are in accordance with the previous studies which have shown that UAE cam be used to extract higher contents of bioactive compounds than other conventional extraction techniques from *Garcinia indica* (Selvaraj et al., 2022), *Celastrus hindsii* (Pham et al., 2020), *Olea europaea* (Wang et al., 2018), *Potentilla fruticosa* L (Xue et al., 2022).

The second-order polynomial equation model was used to fit the experimental outputs (Cheng et al., 2008). The resulting regression equation underwent an ANOVA analysis. The significance of the coefficient was established at a 95% confidence level using the F test and p value. The F test results highlighted the significance of each coefficient variable, whilst the resulting p values highlighted the significance of the interaction between the parameters. If the p value decreases while the F value increases, this would be determined (Atkinson et al., 2007). Particularly, when the p values are less than 0.05, 0.01 and 0.001, the model terms are portrayed as being significant, extremely significant, and impressively significant, respectively (Cao et al., 2021). And with p values more than 0.05, the model terms are non-significant. In this study, the observed values $F = 2.55$ and $p \leq 0.05$; hence, the planned model was highly significant. Multiple regression coefficients (R^2) and the significance of lack of fit determine the fitness and adequacy of the model (Heydarian et al., 2017). Additionally, a best model fit was found for the multiple regression coefficients (R^2) of TP, TF, and antioxidant potentials (% DPPHsc, % ABTSsc, and $\%H_2O_2$sc), which were 0.7038, 0.7061, 0.7697, 0.7482, and 0.7197, respectively. The R^2 adjusted close to the R^2 assured to a good fit of the quadratic models to the experimental data (Shin and Lee, 2021). This suggested that 95% of the actual levels match those predicted by the model.

Investigation of the model

Total polyphenols content (TP)

Table 3 and the second order polynomial Eq. (8) demonstrated the linear terms of methanol concentration (X_1), particle size (X_4), interaction term X_1X_4 and quadratic terms X_2^2, X_3^2 are illustrated as significant ($<<0.05$) contributions of the maximum yield of TP. The correlation coefficient (R^2) value of UAE of TP in the predicting model was 0.7038 with p value of lack of fit was 0.7973, signifying a best correlation between experimental and predicted data. The obtained experiential values are measured to be significant and to found the model is a fitting one. Further, the second–order polynomial equation for the fitted quadratic model for TP in coded variables are presented in below Eq. (8).

Table 3 Analysis of variance (ANOVA) for the quadratic polynomial mode

Source	Sum of squares	df[a]	Mean square	F-value[b]	*p*-value[c]
TP (y_1)[d]					
Model	82,305.9	14	5878.99	2.55	0.0416
X_1	31,320.38	1	31,320.38	13.56	0.0022
X_2	2242.67	1	2242.67	0.971	0.3401
X_3	805.04	1	805.04	0.3485	0.5637
X_4	4959.38	1	4959.38	2.15	0.1635
X_1X_2	885.06	1	885.06	0.3832	0.5452
X_1X_3	342.25	1	342.25	0.1482	0.7057
X_1X_4	7700.06	1	7700.06	3.33	0.0878
X_2X_3	702.25	1	702.25	0.304	0.5895
X_2X_4	280.56	1	280.56	0.1215	0.7323
X_3X_4	2025	1	2025	0.8767	0.3639
X_1^2	15,000.07	1	15,000.07	6.49	0.0223
X_2^2	4762.57	1	4762.57	2.06	0.1715
X_3^2	4321.5	1	4321.5	1.87	0.1915
X_4^2	2680.36	1	2680.36	1.16	0.2984
Residual	34,645.44	15	2309.7		
Lack of fit	18,285.06	10	1828.51	0.5588	0.7973
Pure error	16,360.38	5	3272.08		
Cor total	117,000	29			
TF (y_2)[e]					
Model	71,489.65	14	5106.4	2.57	0.0399
X_1	26,893.31	1	26,893.31	13.55	0.0022
X_2	1517.45	1	1517.45	0.7648	0.3956
X_3	725.04	1	725.04	0.3654	0.5545
X_4	3623.06	1	3623.06	1.83	0.1966
X_1X_2	1400.03	1	1400.03	0.7056	0.4141
X_1X_3	248.92	1	248.92	0.1255	0.7281
X_1X_4	5328.33	1	5328.33	2.69	0.1221
X_2X_3	176.54	1	176.54	0.089	0.7696
X_2X_4	91.26	1	91.26	0.046	0.8331
X_3X_4	624.38	1	624.38	0.3147	0.5831
X_1^2	14,458.34	1	14,458.34	7.29	0.0165
X_2^2	3229.13	1	3229.13	1.63	0.2214
X_3^2	5597.62	1	5597.62	2.82	0.1137
X_4^2	3386.45	1	3386.45	1.71	0.2111
Residual	29,760.69	15	1984.05		
Lack of fit	16,411.45	10	1641.15	0.6147	0.7605
Pure error	13,349.24	5	2669.85		
Cor total	101,000	29			
DPPHsc (y_3)[f]					
Model	7681.61	14	548.69	3.58	0.0098
X_1	4376.28	1	4376.28	28.56	< 0.0001
X_2	47.15	1	47.15	0.3077	0.5873
X_3	9.97	1	9.97	0.0651	0.8021
X_4	4.86	1	4.86	0.0317	0.861
X_1X_2	83.4	1	83.4	0.5443	0.472
X_1X_3	110.69	1	110.69	0.7224	0.4087
X_1X_4	432.59	1	432.59	2.82	0.1136
X_2X_3	43.43	1	43.43	0.2834	0.6023
X_2X_4	409.79	1	409.79	2.67	0.1228
X_3X_4	447.13	1	447.13	2.92	0.1082
X_1^2	1186.57	1	1186.57	7.74	0.0139
X_2^2	22.66	1	22.66	0.1479	0.706
X_3^2	227.67	1	227.67	1.49	0.2417
X_4^2	92.98	1	92.98	0.6068	0.4481
Residual	2298.36	15	153.22		
Lack of fit	1639.62	10	163.96	1.24	0.4279
Pure error	658.74	5	131.75		
Cor total	9979.98	29			
ABTSsc (y_4)[g]					
Model	4455.22	14	318.23	3.18	0.0166
X_1	2226.71	1	2226.71	22.27	0.0003
X_2	28.47	1	28.47	0.2847	0.6014
X_3	26.34	1	26.34	0.2635	0.6152
X_4	8.73	1	8.73	0.0874	0.7716
X_1X_2	55.97	1	55.97	0.5598	0.4659
X_1X_3	170.19	1	170.19	1.7	0.2116
X_1X_4	239.72	1	239.72	2.4	0.1423
X_2X_3	0.1917	1	0.1917	0.0019	0.9657
X_2X_4	246.59	1	246.59	2.47	0.1371
X_3X_4	319.16	1	319.16	3.19	0.0942
X_1^2	747.1	1	747.1	7.47	0.0154
X_2^2	39.86	1	39.86	0.3987	0.5373
X_3^2	151.95	1	151.95	1.52	0.2366
X_4^2	59.21	1	59.21	0.5922	0.4535
Residual	1499.61	15	99.97		
Lack of fit	920.47	10	92.05	0.7947	0.6471
Pure error	579.14	5	115.83		
Cor total	5954.82	29			
H_2O_2sc (y_5)[h]					
Model	6813.23	14	486.66	2.75	0.0309
X_1	3316.1	1	3316.1	18.71	0.0006
X_2	33.57	1	33.57	0.1894	0.6696
X_3	24.12	1	24.12	0.1361	0.7174
X_4	25.92	1	25.92	0.1463	0.7075
X_1X_2	19.34	1	19.34	0.1091	0.7457
X_1X_3	125.29	1	125.29	0.707	0.4137
X_1X_4	101.34	1	101.34	0.5718	0.4613
X_2X_3	174.75	1	174.75	0.9861	0.3365
X_2X_4	484.5	1	484.5	2.73	0.119
X_3X_4	482.64	1	482.64	2.72	0.1197
X_1^2	1085.88	1	1085.88	6.13	0.0257
X_2^2	362.73	1	362.73	2.05	0.173
X_3^2	185.08	1	185.08	1.04	0.323
X_4^2	114.74	1	114.74	0.6474	0.4336
Residual	2658.26	15	177.22		

Table 3 (continued)

Source	Sum of squares	df[a]	Mean square	F-value[b]	*p*-value[c]
Lack of fit	1893.94	10	189.39	1.24	0.43
Pure error	764.33	5	152.87		
Cor total	9471.49	29			

[a]Degrees of freedom

[b]Test for comparing model variance with residual (error) variance

[c]Probability of seeing the observed F value if the null hypothesis is true

[d]Std Dev: 48.06; Mean: 218.13

[e]Std Dev: 44.54; Mean: 192.52

[f]Std Dev: 12.38; Mean: 47.48

[g]Std Dev: 10.00; Mean: 39.44

[h]Std Dev: 13.31; Mean: 40.80

$$\begin{aligned} \mathrm{TP}(y_1) = &+ 212.10 + 36.13X_1 + 9.67X_2 \\ &+ 5.79X_3 - 14.38X_4 + 7.44X_1X_2 - 4.62X_1X_3 \\ &- 21.94X_1X_4 + 6.63X_2X_3 - 4.19X_2X_4 \\ &- 11.25X_3X_4 + 23.39X_1^2 - 13.18X_2^2 - 12.55X_3^2 + 9.89X_4^2 \end{aligned} \quad (8)$$

Figure 1(A) demonstrate the normal percentage probability plot for studentized residuals of X_1, X_2, X_3 and X_4 and these variants are normally distributed and have zero deviation. Additionally, the predicted data versus experimental data exhibited a greater R^2 value (0.7038) related to RSM's adjusted R^2 value (0.4273). Figure 1(B) displays the high values of the regression coefficient ($R^2 \gg 0.7$) regarded as a good fit. Figure 1(C), and (D) show 3D response surface and 2D contour plot demonstrating the considerable influence of methanol concentration and irradiation time in optimizing the better yield of TP. The yield of TP from *H. indicus* (L.) R.Br. extracts of various experiments presented in Table 2 varied from 101.85 to 352.85 mg gallic acid equivalents (GA)/g. Highest content of TP was attained at a methanol concentration of 60%, temperature of 40 °C, extraction time of 20 min, and particle size 0.5 mm, whereas the lowest content was found at methanol concentration 55%, temperature 40 °C, extraction time 15 min, and particle size 0.5 mm. The highest yield of TP was influenced by temperature and methanol concentration; a higher content of TP was connected with the least particle size with higher methanol concentration. Slight heating may loosen the plant tissue, compromise the strength of cell walls, and increase the solubility of phytochemicals, enabling more compounds to dissolve in the solvent. However, prolonged exposure to ultrasonic waves at a higher temperature may cause phytochemicals to degrade.

Total flavonoids content (TF)

Table 3 and the second order polynomial Eq. (9) demonstrated the linear terms of methanol concentration (X_1), particle size (X_4), interaction term X_1X_4 and quadratic terms X_2^2, X_3^2 are illustrated as significant ($<<0.05$) contributions of the maximum extraction yield of TF. As shown by the response surface analysis of the extract's TF content, which showed a high regression coefficient value $R^2 = 0.7061$ and a p value for lack of fit of 0.7605, the experimental model fits the data well. Additionally, the below equation provides the second-order polynomial equation for the quadratic model fit for the TF in coded variables (9).

$$\begin{aligned} \mathrm{TF}(y_2) = &+ 183.38 + 33.47X_1 + 7.95X_2 + 5.50X_3 \\ &- 12.29X_4 + 9.35X_1X_2 - 3.94X_1X_3 \\ &- 18.25X_1X_4 + 3.32X_2X_3 + 2.39X_2X_4 \\ &- 6.25X_3X_4 + 22.96X_1^2 - 10.85X_2^2 \\ &- 14.29X_3^2 + 11.11X_4^2 \end{aligned} \quad (9)$$

The studentized residuals for X_1, X_2, X_3, and X_4 are shown in Fig. 1(E), and these variants have a normal distribution, and there is no deviation. Figure 1(F) displayed the high values of regression coefficient ($R^2 \gg 0.7$) considered as a good fit. In addition, 3D response surface and the contour plot in Fig. 1(G), and (H) explain the effects of methanol concentration and particle size influence the highest content of TF in the extract. Table 2 varied from 92.9252 to 303.578 mg/rutin equivalents (RU)/g of TF. The maximum yield of TF was obtained at 60% of methanol (v/v), and 0.5 mm of particle size, while the lowest content was obtainable at 55% of methanol, 40 °C, 15 min and 0.5 mm particle size.

Antioxidant potentials (%DPPHsc, %ABTSsc and %H_2O_2)

According to the statistical values of the RSM design in Table 3 and model Eqs. (10)–(12), the linear term of methanol concentration (X_1), and quadratic terms of X_2^2, and X_3^2 have substantial effects on all three antioxidant potentials (%DPPHsc, %ABTSsc, and %H_2O_2sc). In addition, the interaction terms X_2X_4, X_3X_4 have also significantly ($p<0.05$) influenced the H_2O_2* radical scavenging potentials. The models in %DPPHsc, %ABTSsc, and %H_2O_2sc have correlation coefficients (R^2) of 0.7697, 0.7482, and 0.7197, respectively; the corresponding p values for lack of fit were 0.4279, 0.6471, and 0.4300. The observed value indicated that the model fits the data very well. The second-order polynomial equation for the fitted quadratic models for %DPPHsc, %ABTSsc, %H_2O_{2sc} in coded variables are given in Eqs. (10)–(12).

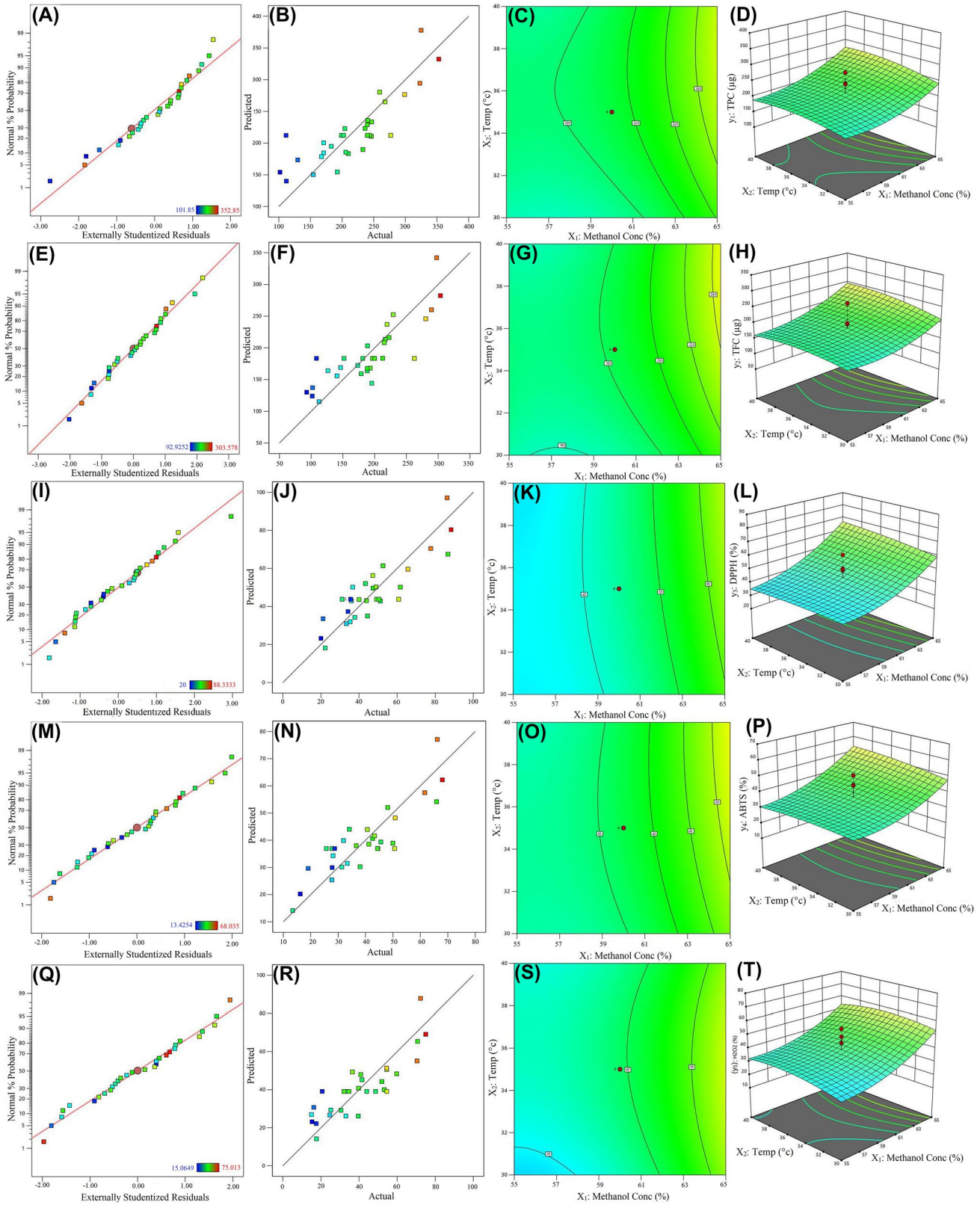
(A)
Normal % Probability
Externally Studentized Residuals
101.85
352.85
(B)
Predicted
Actual
(C)
X2: Temp (°c)
X1: Methanol Conc (%)
(D)
y1: TPC (µg)
X2: Temp (°c)
X1: Methanol Conc (%)
(E)
Normal % Probability
Externally Studentized Residuals
92.9252
303.578
(F)
Predicted
Actual
(G)
X2: Temp (°c)
X1: Methanol Conc (%)
(H)
y2: TFC (µg)
X2: Temp (°c)
X1: Methanol Conc (%)
(I)
Normal % Probability
Externally Studentized Residuals
20
88.3333
(J)
Predicted
Actual
(K)
X2: Temp (°c)
X1: Methanol Conc (%)
(L)
y3: DPPH (%)
X2: Temp (°c)
X1: Methanol Conc (%)
(M)
Normal % Probability
Externally Studentized Residuals
13.4254
68.035
(N)
Predicted
Actual
(O)
X2: Temp (°c)
X1: Methanol Conc (%)
(P)
y4: ABTS (%)
X2: Temp (°c)
X1: Methanol Conc (%)
(Q)
Normal % Probability
Externally Studentized Residuals
15.0649
75.013
(R)
Predicted
Actual
(S)
X2: Temp (°c)
X1: Methanol Conc (%)
(T)
X2: Temp (°c)
X1: Methanol Conc (%)

◂**Fig. 1** Normal percentage probability plot for the studentized residuals for highest yield of TP (**A**), TF (**E**), %DPPHsc (**I**), %ABTSsc (**M**) and $\%H_2O_2$sc (**Q**). Relationship between experimental and predicted value for highest yield of TP (**B**), TF (**F**) %DPPHsc (**J**), %ABTSsc (**N**) and $\%H_2O_2$sc (**R**), Response surface and contour plot showing the combined effects of methanol concentration (X_1) and temperature (X_2) for highest yield of TP, TF, %DPPHsc, %ABTSsc and $\%H_2O_2$sc when time and particle size were held at fixed level (zero level = time 20 min and a particle size of 0.50 mm) (**C**), (**G**), (**K**), (**O**), (**S**) and (**D**), (**H**), (L.), (**P**), (**T**), respectively

$$\begin{aligned}\%\mathrm{DPPHsc}(y_3) &= +43.78 + 13.50X_1 + 1.40X_2 + 0.6446X_3 \\ &\quad + 0.4502X_4 + 2.28X_1X_2 - 2.63X_1X_3 \\ &\quad - 5.20X_1X_4 + 1.65X_2X_3 - 5.06X_2X_4 \\ &\quad - 5.29X_3X_4 + 6.58X_1^2 - 0.9088X_2^2 \\ &\quad - 2.88X_3^2 + 1.84X_4^2 \end{aligned} \tag{10}$$

$$\begin{aligned}\%\mathrm{ABTSsc}(y_4) &= +36.94 + 9.63X_1 + 1.09X_2 + 1.05X_3 \\ &\quad + 0.6032X_4 + 1.87X_1X_2 - 3.26X_1X_3 \\ &\quad - 3.87X_1X_4 + 0.1095X_2X_3 - 3.93X_2X_4 \\ &\quad - 4.47X_3X_4 + 5.22X_1^2 - 1.21X_2^2 \\ &\quad - 2.35X_3^2 + 1.47X_4^2 \end{aligned} \tag{11}$$

$$\begin{aligned}\%\mathrm{H_2O_2sc}(y_4) &= +39.11 + 11.75X_1 + 1.18X_2 + 1.0058X_3 \\ &\quad - 1.04X_4 - 1.10X_1X_2 - 2.80X_1X_3 - 2.52X_1X_4 \\ &\quad + 3.30X_2X_3 - 5.50X_2X_4 - 5.49X_3X_4 \\ &\quad + 6.29X_1^2 - 3.64X_2^2 - 2.60X_3^2 + 2.05X_4^2 \end{aligned} \tag{12}$$

Studentized residuals for X_1, X_2, X_3, and X_4 and these variants fit a normal distribution with no outliers, as shown by a normal percentage probability plot, as shown in Fig. 1(I), (M) and (Q). In addition, Fig. 1(J), (N) and (R) and the predicted data against experimental data for all three antioxidant activities (%DPPHsc, %ABTSsc and $\%H_2O_2$sc) produced higher R^2 values of 0.7697, 0.7482 and 0.7197, respectively, as compared to RSM's adjusted R^2 value, 0.5548, 0.5131 and 0.4574, respectively, and the high values of the regression coefficient ($R^2 \gg 0.7$) is indicating a good fit. Figure 1(K), (O), (S), and (L.), (P), and (T) display the 3D response surface plots and 2D contour plots for three antioxidant activities with methanol concentration (X_1) and particle size (X_4) serving as the relevant functional variables. Figure 1 demonstrate that the maximum antioxidant activities (%DPPHsc, %ABTSsc and FRAP) correspond to the methanol concentration of 65%, and plant material particle size of 0.5 mm. The highest yields of antioxidant potentials are 81.333% for DPPHsc, 65.035% for ABTSsc and 71.013% for H_2O_2sc.

ANFIS modelling analysis

ANFIS modelling was performed for further analysis of extraction parameters, using the same 30 experimental data sets, and it predicted the efficient extraction parameters of polyphenolic compounds from *H. indicus* (L.) R.Br. Table 3 displays the outcomes that were attained in ANFIS. Initially, all the data was randomized. Later, sets were divided for use in the training, testing, and validation of model data. ANFIS was trained in MATLAB v R2013a using the fuzzy logic toolbox in order to obtain the findings. A FIS of ANFIS model with membership functions, 5 outputs, and 4 inputs was built with numerous parameters verified to ensure accuracy (one at a time). Each of the input variables, such as methanol concentration, temperature, time, and particle size, has one of three fuzzy sets: low, medium, or high. The predicted output responses for TP (336 mg GA/g), TF (291 mg RU/g), DPPHsc (81.3%), ABTSsc (65%) and H_2O_2sc (71%) were specified in five fuzzy sets, namely very high, high, medium, low and very low, in accordance with experimental data. In fuzzy inference system, there were 144 network nodes and 36 fuzzy rules. The fuzzy rule was developed using data from experiments and human experiences. The predicted values of the responses were utilised to improve the fuzzy rules through RSM.

Validation of the model

Based on the results from RSM, the optimized extraction parameters were validated for the TP, TF and antioxidant activity (%DPPH, %ABTS, and $\%H_2O_2$ radicals scavenging). The validation experiments were performed using Design Expert software, which was able to recognize the best extraction parameters and their combinations. Additionally, the optimized conditions were also confirmed through ANFIS model using the same data. Validation experiments were performed under optimum conditions, with slight changes based on a combination of responses, and the results are depicted in Supplementary Table 2. The outcomes of the experiment demonstrated that the highest yield of bioactive compounds from *H. indicus* (L.) R.Br. was significantly influenced by the methanol concentration (X_1) and particle size (X_4) of the plant materials. Based on those optimal extraction conditions, a methanol concentration of 62.5–67.5%, a temperature of 37.5–42.5 °C, at a fixed time duration 20 min, and a particle of 0.25–0.5 mm. Under this circumstances, while the experimental values of TP, TF, %DPPHsc, %ABTSsc, and %H2O2sc potentials were 356.67 mg gallic acid equivalents (GA)/g), 312.487 mg rutin equivalents (RU)/g, 88.678%, 68.653% and 76.893%

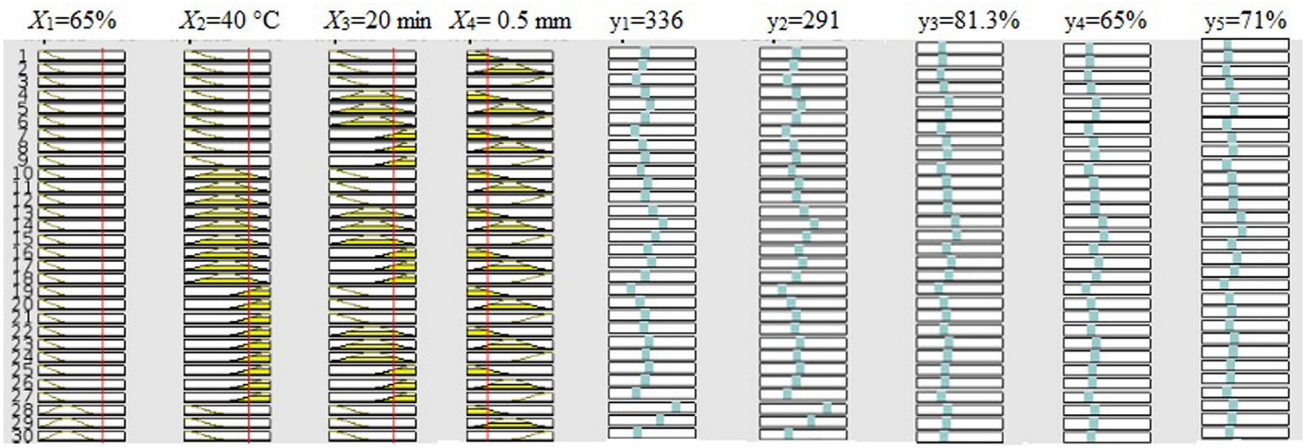

Fig. 2 ANFIS rule viewer for the effect of extraction parameters on responses for extraction of TP, TF and antioxidants from *H. indicus* (L.) R.Br. extract

respectively, RSM's predicted values of TP, TF, %DPPHsc, %ABTSsc, and %H2O2sc potentials were 392.082 mg gallic acid equivalents (GA)/g), 339.625 mg rutin equivalents (RU)/g, 97.7527%, 74.7964% and 82.1651%, respectively. The value of responses was observed using rule viewer plot (Fig. 2) by varying the process variables. The rule viewer is a condensed toolbox that includes built-in algorithms for both fuzzifying input parameters and optimizing neural weights. (Wong et al., 2020). The rule viewer plot tool predicted response variables for model inputs. Experiments and model predictions were compared to cross-verify the model. ANFIS model responses for *H. indicus* (L.) R.Br. extract were 247 mg gallic acid equivalents (GA)/g, 214 mg rutin equivalents (RU)/g, 59.5%, 46.9%, and 53.1% at optimized extraction parameters (methanol concentration = 67.5%, temperature = 40 °C, time = 20 min, and particle size 0.5 mm). Experimental values matched RSM and ANFIS predictions.

GC–MS and LC–MS analysis

The GC–MS chromatogram of optimized extract of *H. indicus* (L.) R.Br. discovered a total of seventeen peaks corresponding to the bioactive chemicals (Fig. 3) that were identified by relating their peaks, retention time, peak area percentage, and molecular mass spectral fragmentation patterns to that of the known compounds designated by the National Institute of Standards and Technology (NIST) library. Among the identified chemicals, methanamine, γ-sitosterol, androstan-17-one, squalene, and beta-amyrin have urinary antiseptic (Josiane et al., 2021) and antioxidant activities, reduces cholesterol and control hyperglycaemia (Tripathi et al., 2013) and triglyceride levels in blood (Lozano-Grande et al., 2018). They also exhibit anti-inflammatory, antinociceptive, gastroprotective and hepatoprotective properties (Melo et al., 2010). The LC–MS chromatogram of methanolic extract of *H. indicus* (L.) R.Br. is presented in Supplementary Fig. 2. The LC–MS chromatogram (Supplementary Fig. 3) showed numerous peaks at different retention times and indicated the presence of five phenolic compounds, namely, emidine (retention time: 12.037 min; molecular formula: $C_{39}H_{64}O_{12}$; mass 724.4398 g/m), denicunine (retention time: 6.690 min; molecular formula: $C_{35}H_{58}O_{10}$; mass: 638.4030 g/m), lupeol (retention time: 20.769 min; molecular formula: $C_{30}H_{50}O$; mass: 426.72 g/m), 3-hydroxy-4-methoxybenzaldehyde (Isovanillin) (retention time: 3.383 min; molecular formula: $C_8H_8O_3$; mass: 152.15 g/m), and 2-hydroxy-4-methoxybenzoic acid (retention time: 1.731 min; molecular formula: $C_8H_8O_4$; mass: 168.15 g/m).

In conclusion, this study reports the optimal extraction parameters of the maximum yield of total polyphenols content, total flavonoids content and their antioxidant potentials (%DPPHsc, %ABTSsc and %H_2O_2sc) from *H. indicus* (L.) R.Br. in the UAE process. The primary extraction parameters ***impacting the UAE were optimized using a statistical method of analysis based on RCCD of RSM and ANFIS modelling. Under these optimal conditions, a maximum yield of TP (y_1) = 352.85 mg gallic acid equivalents per gram (GA/g), TF (y_2) = 300.204 mg rutin equivalents per gram (RU/g) and their antioxidant potentials (%DPPHsc (y_3) = 81.33%, %ABTSsc (y_4) = 65.04%, and %H_2O_2sc (y_5) = 71.01%) were obtained at methanol concentration (X_1) = 65%, temperature (X_2) = 40 °C, time (X_3) = 20 min and particle size (X_4) = 0.5 mm. The identified optimal values were verified and confirmed through second-order polynomial equations and fitting the experimental values as well as the predicted values. A total of 17 and 5 bioactive compounds were identified

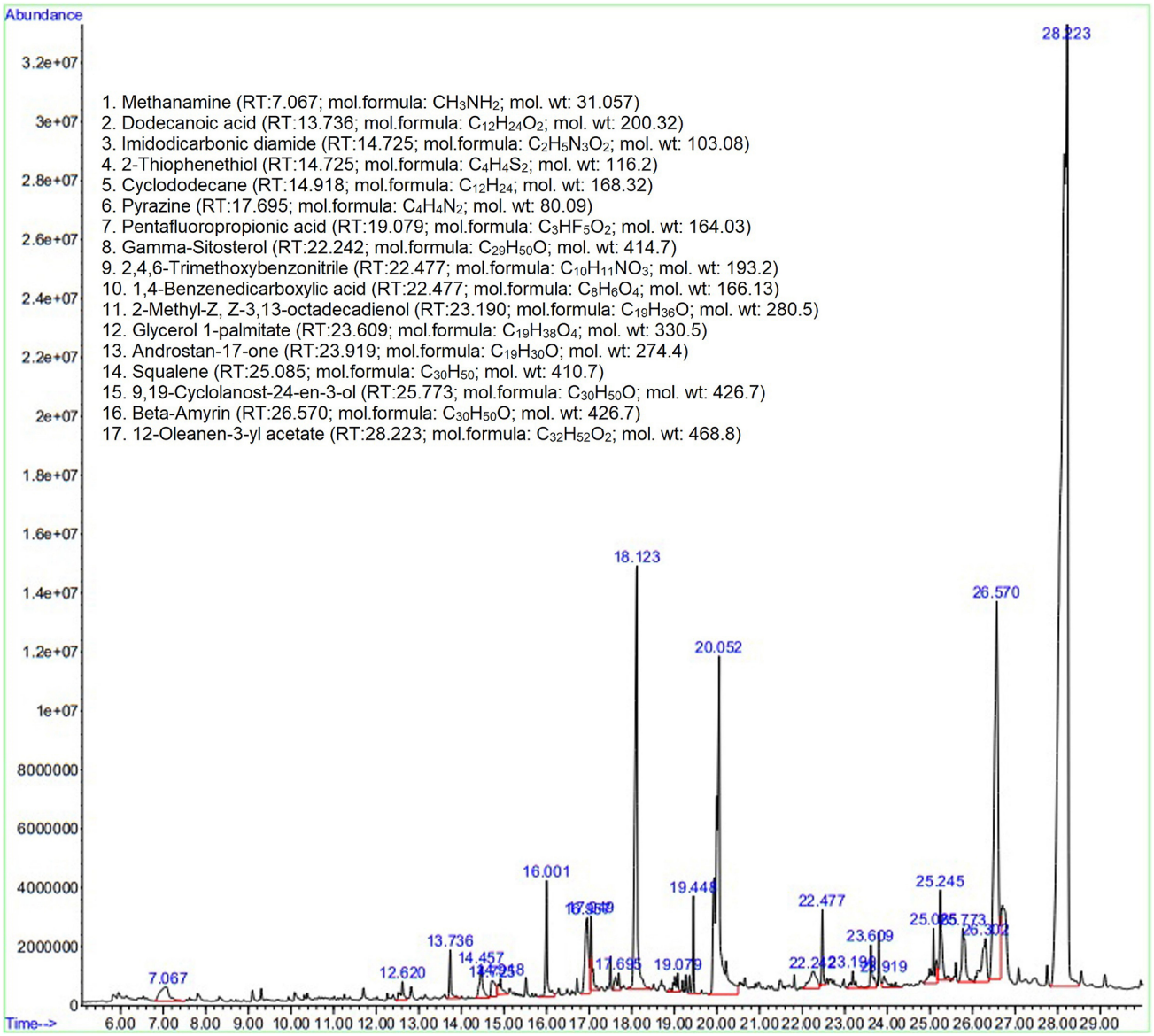

Fig. 3 GC–MS spectra of optimally optimized root extract of *H. indicus* (L.) R.Br. List of bioactive compounds presence in the optimally obtained extract

in the optimally obtained extract of *H. indicus* (L.) R.Br. through GC–MS and LC–MS analysis, respectively.

Supplementary Information The online version contains supplementary material available at https://doi.org/10.1007/s10068-023-01351-9.

Acknowledgements The authors are grateful to the Management of Kalasalingam Academy of Research and Education for the research facilities.

Funding SK and SV gratefully acknowledge the Management of Kalasalingam Academy of Research and Education for Seed Money Grant (KARE/VC/R&D/SMPG/2021-2022/1) and Research Fellowship respectively.

Declarations

Conflict of interest The authors declare that they have no Conflict of interests.

Ethical approval Ethical approval was not required for this research.

References

Al-Mahasneh M, Aljarrah M, Rababah T, Alu'datt M. Application of hybrid neural fuzzy system (ANFIS) in food processing and technology. Food Engineering Reviews. 8(3): 351-366 (2018)

Atkinson A, Donev A, Tobias R. Optimum experimental designs, with SAS, vol 34. Oxford University Press, Oxford (2007)

Baskararaj S, Theivendren P, Palanisamy P, Kannan S, Pavadai P, Arunachalam S, Sankaranarayanan M, Mohan UP, Ramasamy L, Kunjiappan S. Optimization of bioactive compounds extraction assisted by microwave parameters from *Kappaphycus alvarezii* using RSM and ANFIS modeling. Journal of Food Measurement and Characterization. 13: 2773-2789 (2019)

Boominathan P, Chittibabu C, Sivaraj C, Gayathiri E, Arumugam P. Antioxidant, antibacterial and GC-MS analysis of methanol root extract of *Hemidesmus indicus* (L.) R. Br. Journal of Pharmacognosy and Phytochemistry. 7: 1620-1626 (2018)

Brand-Williams W, Cuvelier M-E, Berset C. Use of a free radical method to evaluate antioxidant activity. LWT-Food Science and Technology. 28: 25-30 (1995)

Burton GJ, Jauniaux E. Oxidative stress. Best practice & research Clinical Obstetrics & Gynaecology. 25: 287-299 (2011)

Cao Q, Yan J, Sun Z, Gong L, Wu H, Tan S, Lei Y, Jiang B, Wang Y. Simultaneous optimization of ultrasound-assisted extraction for total flavonoid content and antioxidant activity of the tender stem of *Triarrhena lutarioriparia* using response surface methodology. Food Science and Biotechnology. 30: 37-45 (2021)

Cheng L, Xiong J, He L. Non-Gaussian statistical timing analysis using second-order polynomial fitting. IEEE Transactions on Computer-Aided Design of Integrated Circuits and Systems. 28: 130-140 (2008)

Chowdhury A, Panneerselvam T, Kannan S, Bhattachejee C, Somasundaram B, Sankaranarayanan M, Baskararaj S, Kunjiappan S. Optimization of microwave-assisted extraction of bioactive polyphenolic compounds from *Marsilea quadrifolia* L. using RSM and ANFIS modelling. Indian Journal of Natural Products and Resources (IJNPR)[Formerly Natural Product Radiance (NPR)]. 9: 204-221 (2018)

Chowdhury A, Selvaraj K, Bhattacharjee C, Chowdhury R. Optimization of the solvent extraction of phenolics and antioxidants from waste Cauliflower leaves (*Brassica oleracea* L.) using Response Surface Methodology (RSM). International Journal of Biological Sciences and Technology. 5: 4-12 (2013)

Deshmukh MM, Ambad CS, Kendre N, Kashid NG. Biochemical screening, antibacterial and GC-MS analysis of ethanolic extract of *Hemidesmus indicus* (L.) R. Br. root. Research Journal of Pharmacognosy and Phytochemistry. 11: 73-80 (2019)

Forni C, Facchiano F, Bartoli M, Pieretti S, Facchiano A, D'Arcangelo D, Norelli S, Valle G, Nisini R, Beninati S. Beneficial role of phytochemicals on oxidative stress and age-related diseases. BioMed Research International. 2019 (2019)

Ganesan V, Gurumani V, Kunjiappan S, Panneerselvam T, Somasundaram B, Kannan S, Chowdhury A, Saravanan G, Bhattacharjee C. Optimization and analysis of microwave-assisted extraction of bioactive compounds from *Mimosa pudica* L. using RSM & ANFIS modeling. Journal of Food Measurement and Characterization. 12: 228–242 (2018)

Heydarian M, Jooyandeh H, Nasehi B, Noshad M. Characterization of Hypericum perforatum polysaccharides with antioxidant and antimicrobial activities: optimization based statistical modeling. International Journal of Biological Macromolecules. 104: 287-293 (2017)

Hosseinzadeh S, Jafarikukhdan A, Hosseini A, Armand R. The application of medicinal plants in traditional and modern medicine: a review of *Thymus vulgaris*. International Journal of Clinical Medicine. 6: 635-642 (2015)

Jayalakshmi B, Kruthika L, Amruthesh K. Phytochemical study and antioxidant property of (L.) R. Br. roots *Hemidesmus indicus*. Asian Journal of Pharmacy and Pharmacology. 4: 719–723 (2018)

Josiane KNG, Raphaël KJ, Ruben NT, Divine YMD, Agwa ED, Gilchrist TD, Valdes NTB, Issa IB. Effects of methenamine feeding regime on growth performances, gut microbiota, organs histology and haemato-biochemical profile of broiler chickens. Open Journal of Animal Sciences. 11: 238-254 (2021)

Kharat T, Mokat D. Pharmacognostic and phytochemical studies on *Hemidesmus indicus* and its substitute *Decalepis hamiltonii*—Review. International Journal of Botany Studies. 5: 224-231 (2020)

Kovacic P, Jacintho JD. Reproductive toxins pervasive theme of oxidative stress and electron transfer. Current Medicinal Chemistry. 8: 863-892 (2001)

Lobo V, Patil A, Phatak A, Chandra N. Free radicals, antioxidants and functional foods: Impact on human health. Pharmacognosy Reviews. 4: 118-126 (2010)

Lozano-Grande MA, Gorinstein S, Espitia-Rangel E, Dávila-Ortiz G, Martínez-Ayala AL. Plant sources, extraction methods, and uses of squalene. International Journal of Agronomy. 2018 (2018)

Melo CM, Carvalho KMMB, de Sousa Neves JC, Morais TC, Rao VS, Santos FA, de Castro Brito GA, Chaves MH. α, β-amyrin, a natural triterpenoid ameliorates L-arginine-induced acute pancreatitis in rats. World Journal of Gastroenterology: World Jourrnal of Gasteroenterology. 16: 4272-4280 (2010)

Nayar R, Shetty J, Mary Z, Yoganarasimhan S Pharmacognostical studies on the root ofDecalepis hamiltonii Wt. and Arn., and comparison with *Hemidesmus indicus* (L.) R. Br. In: Proceedings of the Indian Academy of Sciences-Section B, 1978. vol 2. Springer, pp 37–48

Pham D-C, Nguyen H-C, Nguyen T-HL, Ho H-L, Trinh T-K, Riyaphan J, Weng C-F. Optimization of ultrasound-assisted extraction of flavonoids from Celastrus hindsii leaves using response surface methodology and evaluation of their antioxidant and antitumor activities. BioMed Research International. 2020 (2020)

Ruch RJ, Cheng S-j, Klaunig JE. Prevention of cytotoxicity and inhibition of intercellular communication by antioxidant catechins isolated from Chinese green tea. Carcinogenesis. 10: 1003–1008 (1989)

Saetan P, Usawakesmanee W, Siripongvutikorn S, Yupanqui CT. Reduction of safrole content of *Cinnamomum porrectum* leaves by blanching and the effect on the antioxidant and anti-inflammatory activities of its herbal tea. Functional Foods in Health and Disease. 7: 936-957 (2017)

Selvaraj K, Chowdhury R, Bhattacharjee C. Isolation and structural elucidation of flavonoids from aquatic fern Azolla microphylla and evaluation of free radical scavenging activity. International Journal of Pharmcy and Pharmaceutical Sciences. 5: 743-749 (2013)

Selvaraj K, Chowdhury R, Bhattacharjee C. Optimization of the solvent extraction of bioactive polyphenolic compounds from aquatic fern *Azolla microphylla* using response surface methodology. International Food Research Journal. 21: 1559-1567 (2014)

Selvaraj K, Theivendren P, Pavadai P, Ravishankar V, Palanisamy P, Gopal M, Dharmalingam SR, Sankaranarayanan M. Impact of physicochemical parameters on effective extraction of bioactive compounds from natural sources: an overview. Current Bioactive Compounds. 18: 11-27 (2022)

Shin K-S, Lee J-H. Optimization of enzymatic hydrolysis of immature citrus (*Citrus unshiu* Marcov.) for flavonoid content and antioxidant activity using a response surface methodology. Food Science and Biotechnology. 30: 663-673 (2021)

Siddhuraju P, Becker K. Antioxidant properties of various solvent extracts of total phenolic constituents from three different agroclimatic origins of drumstick tree (*Moringa oleifera* Lam.) leaves. Journal of Agricultural and Food Chemistry. 51: 2144-2155 (2003)

Singleton VL, Orthofer R, Lamuela-Raventós RM. Analysis of total phenols and other oxidation substrates and antioxidants by means

of folin-ciocalteu reagent. Methods in Enzymology. 299: 152-178 (1999)

Stojanović-Radić Z, Pejčić M, Dimitrijević M, Aleksić A, V. Anil Kumar N, Salehi B, C. Cho W, Sharifi-Rad J (2019) Piperine-a major principle of black pepper: a review of its bioactivity and studies. Applied Sciences. 9: 4270

Tripathi N, Kumar S, Singh R, Singh C, Singh P, Varshney V. Isolation and identification of γ-Sitosterol by GC–MS from the leaves of (Decne). The Open Bioactive Compounds Journal. 4: 25-27 (2013)

Valko M, Leibfritz D, Moncol J, Cronin MT, Mazur M, Telser J. Free radicals and antioxidants in normal physiological functions and human disease. The International Journal of Biochemistry & Cell Biology. 39: 44-84 (2007)

Valko M, Rhodes C, Moncol J, Izakovic M, Mazur M. Free radicals, metals and antioxidants in oxidative stress-induced cancer. Chemico-Biological Interactions. 160: 1-40 (2006)

Vellur S, Pavadai P, Babkiewicz E, Pandian SRK, Maszczyk P, Kunjiappan S. An in silico molecular modelling-based prediction of potential Keap1 inhibitors from *Hemidesmus indicus* (L.) R.Br. against oxidative-stress-induced diseases. Molecules. 28: 4541 (2023)

Wang B, Qu J, Luo S, Feng S, Li T, Yuan M, Huang Y, Liao J, Yang R, Ding C. Optimization of ultrasound-assisted extraction of flavonoids from olive (*Olea europaea*) leaves, and evaluation of their antioxidant and anticancer activities. Molecules. 23: 2513 (2018)

Wong YJ, Arumugasamy SK, Chung CH, Selvarajoo A, Sethu V. Comparative study of artificial neural network (ANN), adaptive neuro-fuzzy inference system (ANFIS) and multiple linear regression (MLR) for modeling of Cu(II) adsorption from aqueous solution using biochar derived from rambutan (*Nephelium lappaceum*) peel. Environmental Monitoring and Assessment. 192: 1-20 (2020)

Xue H, Li J, Wang G, Zuo W, Zeng Y, Liu L. Ultrasound-assisted extraction of flavonoids from *Potentilla fruticosa* L. using natural deep eutectic solvents. Molecules. 27: 5794 (2022)

Zhou Y, Yang W, Li Z, Luo D, Li W, Zhang Y, Wang X, Fang M, Chen Q, Jin X. *Moringa oleifera* stem extract protect skin keratinocytes against oxidative stress injury by enhancement of antioxidant defense systems and activation of PPARα. Biomedicine & Pharmacotherapy. 107: 44-53 (2018)